

GPO PRICE \$ \_\_\_\_\_  
 CFSTI PRICE(S) \$ \_\_\_\_\_  
 Hard copy (HC) \$2.00  
 Microfiche (MF) 1.50  
 # 853 July 65

FACILITY FOR \_\_\_\_\_  
 REPORT NUMBER 38  
 (PAGES)  
 CR-64421  
 (NASA CR OR TMX OR AD NUMBER)  
 (THRU) 1  
 (CODE)  
 12  
 (CATEGORY)

Exploratory Measurements in  
 Spiral Turbulence\*

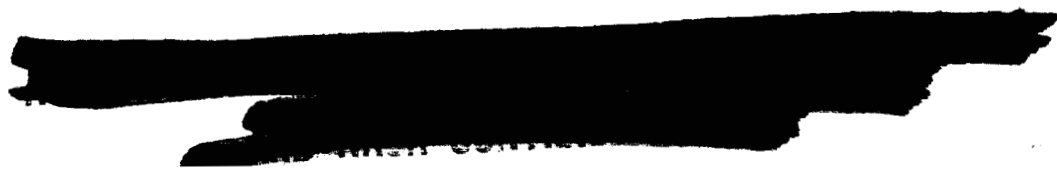
Charles Van Atta  
 Jet Propulsion Laboratory, Pasadena, California

ABSTRACT

27079

The present experiments lay a foundation for a study of interface propagation in a mixed laminar-turbulent flow between counter-rotating concentric cylinders. Such mixed flows, including one particularly well-organized pattern called spiral turbulence, are found to be a dominant feature of transition in Couette flow. In spiral turbulence, the laminar and turbulent regions of the flow form an alternating pattern of helical stripes, rotating with approximately the mean angular velocity of the two cylinders. Stable right- and left-handed spirals occur with equal probability when the flow is established from rest. Hot-wire measurements have been made of the mean cross-sectional shape of the interfaces in the axial mid-plane for a spiral-turbulent flow having low dispersion in interface position. A nose of turbulence associated with the leading interface projects into the laminar region near the outer cylinder, while a corresponding tail is associated with the trailing interface near the inner cylinder. Fluctuations in interface position and in apparent length of the turbulent region are closely Gaussian, and the fluctuations are rapid compared with the period of rotation of either cylinder.

\* This paper presents the results of one phase of research carried out at the Jet Propulsion Laboratory, California Institute of Technology, under Contract No. NAS 7-100, sponsored by the National Aeronautics and Space Administration.



## 1. Introduction

Under certain conditions, a pattern of alternating helical stripes of laminar and turbulent flow can be observed in the gap between concentric rotating cylinders. This phenomenon, now called spiral turbulence, was first observed by Oguro (unpublished) and Coles (1962) in the large rotating-cylinder apparatus at GALCIT\*. Oguro's measurements were made with the inner cylinder at rest and the outer cylinder rotating at high speed. A stable mixed laminar-turbulent configuration was found, with the laminar flow confined to narrow regions near both walls. The pattern rotated with approximately half the angular velocity of the outer cylinder. At about this same time, Coles obtained the photograph shown in Figure 1, using a smaller apparatus and a suspension of aluminum particles in silicone oil as a means of flow visualization. In this case, the cylinders are rotating in opposite directions at relatively low speed. The mottled areas in the photograph indicate turbulent flow, and the smoother areas indicate laminar flow. The helical pattern, which may be either right- or left-handed, again rotated at approximately the mean angular velocity of the two cylinders without changing its general shape.

Oguro's measurements indicated that fluid elements move on the average in nearly circular paths, so that an element near either wall repeatedly traverses the pattern, participating alternately in the laminar and turbulent motion. In any event, it is certain that the volume of turbulent fluid in spiral turbulence is statistically constant. Hence any flow into the turbulent region must be balanced by an equal flow out. Barring the unlikely event that there is no net flow in either direction, it follows that

---

\*Graduate Aeronautical Laboratories, California Institute of Technology



interfaces separating regions of laminar and turbulent flow must be of two kinds. One kind, involving transition in the usual sense, propagates into the laminar region; the other kind, involving inverse or anti-transition, propagates into the turbulent region.

Given this property of spiral turbulence, what is the mechanism by which turbulence disappears at an anti-transition interface? The almost equal sharpness observed for leading and trailing interfaces, as illustrated by a typical hot-wire signal in Figure 2, suggests that this mechanism may not be entirely viscous or diffusive in nature. The present research is part of an attempt to study this question by measuring the local rate of energy transfer between mean flow and turbulence, especially near the interfaces. The experimental technique is both new and difficult, requiring thousands of accurate measurements of the instantaneous velocity vector at each of hundreds of known points in the flow pattern. It was obvious from the beginning that only one such flow could reasonably be studied in the necessary detail. The present Paper describes some exploratory measurements which led to the choice of a particular flow. Although the detailed study of this flow is not yet complete, some progress to date has been summarized by Van Atta (1964).

## 2. Apparatus

The experiments were performed in the large rotating-cylinder apparatus described by Coles (1965). The working fluid is air. The nominal inner and outer diameters of the annular working space are 32 and 36 in. respectively. The axial length of the working space can be varied in the range from 34 to 55 in. by means of adjustable endplates which prevent outside disturbances from propagating into the annulus. The endplates rotate with the outer cylinder, and there is a discontinuity

in velocity [of magnitude  $(\omega_o - \omega_i)r_i$ ] where the endplates meet the inner cylinder. Each cylinder is equipped with a slip ring assembly to allow hot-wire and other signals to commute between laboratory and rotating frames. For the exploratory measurements described here, the hot-wire instrumentation usually consisted of single-wire probes operated at constant current. The stem of each probe was a length of 0.042-in. OD stainless-steel tubing with a 90-deg bend. The tubing served as one electrical conductor. An insulated central conductor of 0.013-in. D drill rod protruded from both ends of the tubing. The hot-wire (0.0001-in. D) was soldered to the pointed tips of this central conductor, and another short length of drill rod soldered to the tube wall. The probes were mounted on aluminum pads, fitting snugly into 0.625-in. D holes in the wall of each cylinder and conforming to the curvature of the cylinder on the face exposed to the flow.

The angular velocity of the outer cylinder, which always rotated in the same direction, was arbitrarily taken as negative. The Reynolds numbers for the outer and inner cylinders  $R_o$  and  $R_i$  take the signs of  $\omega_o$  and  $\omega_i$ , respectively. For most of the experiments, the cylinders turned in opposite directions, and  $\omega_i$  and  $R_i$  were positive.

The intermittency meter, which was designed and constructed by Oguro, had a cathode-ray tube and photo-multiplier tube as basic elements. The lowest frequencies in the hot-wire signal, corresponding to mean-flow variations, were filtered out, and the amplitude of the resulting signal was adjusted until the oscilloscope trace was completely masked (during any laminar intervals) by a thin horizontal strip of opaque tape. Turbulent signals were detected by a photomultiplier tube, looking at the oscilloscope face through a lens system. The output of the photo-multiplier tube,

smoothed by a suitable choice of phosphor for the cathode-ray tube and also by a low-pass filter, was converted to a square wave and used to gate an oscillator signal into a counter during intervals of turbulent flow. To obtain the intermittency factor, the reading of the gated counter was divided by the reading of a second free-running counter driven by the same time base. A half-silvered mirror allowed observation of the partially masked signal without disturbing the discrimination process. The intermittency meter was calibrated by the usual subjective method; i. e., by adjusting the time constants and trigger levels until the gate signals appeared to coincide with the beginning and end of turbulence in the untreated signal.

### 3. Observations of Transition

In the earliest experiments, the angular velocities of the two cylinders were unsystematically increased until transition to fully or partially turbulent flow occurred. Except where noted, the length of the working space was kept fixed at its maximum value of 54.7 in. The flow was normally observed at mid-radius ( $r = 17$  in.) in the axial mid-plane of the cylinders ( $z = 0$ ), using hot-wire probes mounted on either cylinder. As expected, intermittency was found to be the dominant feature of transition when the cylinders turned in opposite directions. For a wide range of Reynolds numbers, the hot-wire signals showed a regular alternation between laminar and turbulent flow, as in Figure 2, or else showed turbulent flow in which the amplitude of the turbulence varied periodically with a comparable frequency. More irregular flows were also observed, in which the laminar and turbulent regions were not as uniformly compartmented. In some instances, a tendency was noted for successive turbulent regions to bunch together, swallowing up the laminar

region. In other cases, turbulence sometimes appeared briefly in the normally laminar portion of the signal. The latter behavior is believed to be due to irregularities in the interface or to rapid fluctuations in interface position, rather than to islands of turbulence separated from the main body of turbulent fluid.

To investigate more closely the manner in which these intermittently turbulent flows were established, the speeds of the cylinders were varied more systematically. With laminar flow in the annulus, and with the Reynolds number  $R_o$  of the outer cylinder held constant, the angular velocity of the inner cylinder was increased slowly from zero in the opposite direction. Provided that  $R_o$  was neither too large nor too small, the flow remained entirely laminar up to a repeatable critical value  $R_{ic}$  at which turbulence appeared with catastrophic suddenness. In some cases, the subsequent signal showed a periodic alternation between laminar and turbulent flow; and in other cases it was fully turbulent, with or without an observable low-frequency variation in amplitude. By making several runs at fixed  $R_o$ , with  $R_i$  increasing as slowly as possible, a lower bound was established for  $R_{ic}$ , as shown in Figure 3.

For  $R_o$  less than about 100,000, this experimental boundary for catastrophic transition follows the trend of the theoretical Taylor instability boundary. In this range, transition is probably caused by breakdown of the toroidal vortices which are known to exist above the Taylor boundary, and to increase in strength as  $R_i$  increases. The Taylor instability itself, since it produces no circumferential flow variation, could not be detected experimentally.

For  $R_o$  greater than about 100,000, a different behavior was found:  $R_{ic}$  decreased to zero as  $R_o$  increased. The stability analysis of

Schultz-Grunow (1959) indicates that flow below the Taylor boundary is also stable to infinitesimal disturbances of Tollmien-Schlichting type. At these higher Reynolds numbers, however, transition may be initiated by either of two finite disturbances that always exist in the flow. These are (a) the vorticity concentration at the endplate, and (b) probe wakes. A very similar transition boundary was observed by Coles (1965), employing a flow visualization technique which avoided probe disturbances. From his visual observations, he concluded that transition began in the vorticity concentrations at the endplates, which were split at mid-radius. In the present experiments, the endplates rotated with the outer cylinder, and the Reynolds number  $-R_o$  at which the influence of the endplates first becomes apparent changed from 40,000 (Coles' data) to 100,000. As may be seen in Figure 3, there is also a small systematic shift in the transition boundary when the length of the working space is decreased by 40%. The latter result is consistent with the study by Coles and Van Atta (1965) showing that the laminar velocity profile at large Reynolds numbers can be profoundly influenced even by relatively distant endplates.

The effect of probe disturbances was not investigated in detail. At three speeds, runs with different radial probe positions showed no significant change in the transition Reynolds number  $R_{ic}$ , suggesting that the probe played no important role in initiating the turbulence. On the other hand, it was found during probe calibrations with the inner cylinder at rest (Coles and Van Atta, 1965) that the wake of a larger multiple hot-wire probe definitely triggered transition when the probe Reynolds number (based on stem diameter and relative velocity at the tip) exceeded a value of about 300.

When  $R_i$  was increased beyond  $R_{ic}$ , the flow became increasingly turbulent ( $\gamma$  increasing). In all cases, a value of  $R_i$  could be reached for which the intermittency factor at mid-gap was unity, and the turbulence was of uniform intensity. When  $R_i$  was first increased to  $R_{ic}$  and then decreased, turbulence persisted, the alternations between laminar and turbulent flow becoming at first more regular and sharply defined. As  $R_i$  was further decreased, both the intervals between bursts of turbulence and the lengths of the bursts became increasingly random, until the turbulence degenerated and disappeared permanently at a lower critical Reynolds number. This lower bound, denoted by the curve  $\gamma = 0$  in Figure 3, was established by varying the speed of the inner cylinder as slowly as possible. For sufficiently large  $R_o$ , intermittency persisted even when both cylinders rotated in the same sense.

The hysteresis just described means that two distinct states (one completely laminar, the other partially or fully turbulent) could be observed for certain values of  $R_o$  and  $R_i$ . The intermittent turbulent flows throughout the transition region, as characterized by the intermittency factor and by the angular velocity of the interfaces (see Section 4) seemed to be unique, no matter how the cylinder speeds approached their equilibrium values. For example, if the angular velocity of the inner cylinder was fixed and the angular velocity of the outer cylinder was increased slowly from rest, transition could occur gradually through a progression of increasingly irregular motions<sup>\*</sup>, but the final state of the flow was the same unique function of the two Reynolds numbers.

---

<sup>\*</sup> Because the transition boundary has a negative slope in Figure 3, catastrophic transition will not be observed when operating in this manner unless  $R_i$  is quite small.



#### 4. Interface Propagation Velocity

In the region of spiral turbulence, the average angular velocity of the interfaces relative to the laboratory  $\omega_t$  and the number of turbulent regions propagating around the annulus  $N$  were calculated from the frequency of the pattern, as observed from probes on both cylinders. Frequencies were obtained by timing thirty or more cycles of the flow pattern with a stopwatch. The relevant expressions, in which  $f_o$  and  $f_i$  are the frequencies of the pattern observed from the outer and inner cylinders, respectively, are;  $\omega_t = (\omega_i f_o + \omega_o f_i) / (f_o + f_i)$  and  $N = 2\pi(f_o + f_i) / (f_o - f_i)$ . In all cases, the number of turbulent regions calculated was unity (to one part in a thousand). The interfaces always travel in the same direction as the outer cylinder, which is rotating faster than the inner cylinder.

As shown in Figure 4, the quantity  $2\omega_t / (\omega_o + \omega_i)$ , although a weak function of Reynolds number over most of the transition region, is nearly equal to unity for most of the observations. In other words,  $\omega_t$  is approximately equal to the mean angular velocity of the two cylinders; the turbulence moves as if it were being convected with the mean angular velocity of the fluid. Above the Taylor boundary, there is a relatively rapid rate of increase in  $2\omega_t / (\omega_o + \omega_i)$ , as exhibited in Figure 4, so that instability of the Taylor type may play a role even after turbulence has become established.

For  $R_o$  less than 100,000, the data in Figure 4 were obtained with hot-wires located at mid-gap, but, for larger values of  $R_o$ , the signals at mid-gap lost their modulated character as the intensity of the turbulence became independent of  $\theta$ . Since the flow near the outer cylinder remained periodically intermittent for larger Reynolds numbers, most of the  $\omega_t$  data for  $R_o > 100,000$  were obtained at  $r = 17.9$  in.

## 5. Evidence for Helical Structure

To determine whether the flow in the large machine had a spiral pattern as in Figure 1, the differences in arrival times of a given interface at three probes having different axial locations were roughly measured for a few cases with  $R_o$  between -18,000 and -60,000. The time intervals were measured from photographic records obtained with a dual-beam oscilloscope or (at the lower speeds) with a stopwatch. The probes were all mounted on the outer cylinder, at  $r = 17$  in. One probe was at  $z = 0$ ,  $\theta = 0$  deg, while the other two probes were located at  $z = -24$  in.,  $\theta = 0$  deg and  $z = -12$  in.,  $\theta = +15$  deg. The hypothetical helix angle was computed from the average time interval between the beginning of successive turbulent bursts in the signals from each pair of probes.

Since the hand of the helix was not known a priori, the helix angle was computed twice, assuming first a left-handed and then a right-handed helix. The angles calculated from different pairs either differed substantially (usually by about 20 deg, or roughly a factor of two) or else were very close together (within 1 or 2 deg in several cases). For two cases in which the calculated angles differed by less than 1 deg, the calculated helix angles were 27.5 and 28.0 deg, measured with respect to a plane  $z = \text{constant}$ . The latter value was for  $R_o = -18,300$ ,  $R_i = 6,370$ , fairly close to the operating point of the smaller machine in Figure 1 ( $R_o = -15,900$ ,  $R_i = 5,300$ ). One full turn of a helix with a pitch angle  $\alpha$  of 28 deg  $\left[ \tan \alpha = (dz/rd\theta)_h \right]$  would have an axial length of 57 in., implying that the helix in the large machine was also wrapped nearly once around the annulus, whose actual length was 54.7 in.

It was found that both right- and left-handed helical patterns had been observed. In one case, measurements taken several minutes apart

showed that the helix had changed hand while both cylinder speeds remained constant. This transition from one hand to the other was observed as a brief period (about 15 sec, or 5 normal cycles of the flow) of very irregular, fully turbulent flow. These measurements were relatively crude, since only about 10 cycles of the flow were used to obtain the average time intervals, but they did confirm both the helical structure of the flow and the existence of right- and left-handed configurations in the large apparatus.

Further evidence for right- and left-handed helices was obtained during a preliminary study of the axial flow component for the optimal spiral-turbulence configuration discussed in Section 6 below. The difference signal from two hot-wires forming a V-array in the surface  $r = 16.5$  in. showed a strongly periodic low-frequency component, with extreme values in the laminar and turbulent portions of the cycle (cf. Figure 2). The sensitivity of the wire array to changes in flow angle was measured by yawing the probe in a laminar flow, and the overall flow deflection per cycle in the spiral turbulence was estimated to be about 10 deg. When the intermittent flow was established repeatedly from rest, it was found that the low-frequency part of the difference signal was sometimes reflected in the horizontal axis, showing the random occurrence of two flows having opposite hands. The two hands deflected the mean flow in opposite directions as corresponding laminar and turbulent regions of the flow pattern were traversed.

## 6. An Optimal Flow

A principal objective of the general transition survey was to find the most regular mixed-flow configuration obtainable with the apparatus, using two criteria: (1) sharply delineated laminar and turbulent regions for all radial locations in the annulus, and (2) low dispersion for

fluctuations of the interface geometry about its mean position in suitable rotating coordinates. A group of extremely stable mixed flows satisfying these criteria was noted in the region  $R_o = -40,000$  to  $-50,000$ ,  $R_i = 3,500$  to  $10,000$ . Visual inspection of hot-wire signals in this region indicated that the most regular flow, and thus the most suitable flow for the elaborate measurements mentioned in Section 1 would be found in the neighborhood of  $R_o = -50,000$ , with  $R_i$  between  $5,000$  and  $6,000$ .

With  $R_o$  fixed at  $-48,000$ , a quantitative measure of the regularity of the flow at various values of  $R_i$  was next obtained by measuring the dispersion in the time interval  $P$  between successive observations of the same interface at  $r = 17$  in. The intermittency meter produced a square wave whose positive going edges marked the beginning of turbulence for each cycle. For several values of  $R_i$ , 300 time intervals between successive pairs of these edges were measured with an electronic counter and recorded manually. The result in each case was a nearly Gaussian distribution function for  $P$ , as shown in Figure 5. (For a normally distributed variable, the scales are arranged to produce a straight line with a slope inversely proportional to the standard deviation). Given the mean period  $\langle P \rangle$  and the standard deviation  $\sigma$ , the ratio  $\sigma/\langle P \rangle$  provides a direct measure of relative dispersion in interface position at different Reynolds numbers, as shown in Figure 6. The brackets in the figure are an estimate of the uncertainty in  $\sigma$  arising from graphical determination of the slope in Figure 5. The plot of  $\sigma/\langle P \rangle$  vs  $R_i$  determines an optimal flow, since there is a minimum near  $R_i = 5,600$ . The operating point  $R_o = -50,000$ ,  $R_i = 5,600$  was therefore chosen for further exploratory measurements. In the neighborhood of this operating point, according to Figure 4, the normalized angular velocity of the turbulence is practically

independent of both  $R_o$  and  $R_i$ . The operating point for the optimal flow also lies in the hysteresis region, approximately halfway between the Taylor boundary and the boundary  $\gamma = 0$  below which turbulence cannot persist. It follows that it is possible, although perhaps not desirable, to establish a laminar flow for probe calibration at precisely the same operating conditions as for the optimal spiral turbulent flow.

#### 7. Intermittency Measurements in the Optimal Flow

For the present measurements, the intermittency factor  $\gamma$  is defined as the fraction of the circumference occupied by turbulent flow as observed with a moving probe at fixed radius. Measurements of the apparent length of the turbulent region, supplemented by correlations of time intervals between successive crossings of the same interface (see Figure 12 and Appendix), indicate that the volume of turbulent fluid is continually changing its shape and size on a time scale considerably less than the time required by the probe to traverse once through the flow pattern. Consequently, no information about the instantaneous shape or length of the turbulent region can be obtained from these measurements.

All measurements of  $\gamma$  reported here were obtained by averaging over at least 100 cycles of the pattern (approximately 5 mins.). The pass band of the  $\gamma$ -meter filter (Kronhite 330-M) was 4 cycles/sec to 20,000 cycles/sec, but there was very little turbulent energy above 200 cycles/sec. For  $R_o = -50,000$ , the variation of  $\gamma$  with  $R_i$ , measured at  $z = 0$  for three different radii, is plotted in Figure 7. With increasing Reynolds number,  $\gamma$  increased more slowly near the walls than in the center of the gap, increasing most slowly near the outer cylinder. Thus the flow can be essentially fully turbulent near the inner cylinder and at mid-gap, while the intermittency factor near the outer cylinder is still as low as 0.7.

With regard to the radial distribution of  $\gamma$ , the flow studied by Oguro ( $R_o = -250,000$ ,  $R_i = 0$ ) was of this type.

The radial distribution of  $\gamma$  at  $z = 0$  for  $R_o = -50,000$ ,  $R_i = 5,600$  (the optimal flow) in Figure 7 shows a broad maximum at mid-gap, around which the distribution is nearly symmetrical. The dispersion in the time interval  $P$  between successive observations of the same interface, and the dispersion in the length of the turbulent region  $\ell_t$ , are generally larger near the walls than in the center of the gap. For three radii, the dispersion in  $\ell_t$  was found by measuring individual intervals during which the intermittency meter indicated turbulent flow. This was accomplished by manually resetting a gated counter to zero during an interval of laminar flow and recording the number displayed on the counter after an interval of turbulent flow. From the approximately Gaussian distribution functions shown in Figure 8, the normalized dispersion in  $\ell_t$  at points 0.1 in. from each wall was estimated to be perhaps 50 to 100% larger than at mid-gap. The intervals between observations of the same interface showed an even larger increase in dispersion near the walls, being nearly 60% larger at  $r = 16.25$  in. than in the center of the gap (Figure 9).

The effect of the length of the working space on the stability and intermittency of the optimal flow at  $R_o = -50,000$ ,  $R_i = 5,600$  was briefly studied by moving both endplates inward to decrease  $L$ , keeping the probe fixed at  $z = 0$ ,  $r = 17$  in. The intermittency factor varied slowly with  $L$ , increasing from 0.58 at the maximum length of 54.7 in. to 0.62 at the minimum length of 34.0 ins. However, there was a striking change in the stability of the interface pattern as  $L$  decreased. The flow was very stable for  $L$  greater than 44 in., but became progressively more irregular as  $L$  was decreased below this value. For the minimum length, the hot-wire

signals typically showed the usual alternation between laminar and turbulent flow for periods of several minutes, and then showed complete turbulence for intervals of 15 to 20 sec (5 to 7 periods of the normal intermittent signal). It was conjectured that decreasing the length of the apparatus increased the tendency for the flow to change hand spontaneously, and this conjecture was later verified by observations during which the hand of the flow was continuously monitored.

For fixed  $\omega_o$  and  $\omega_i$ , the angular velocity of the turbulence increased slightly as the length of the cylinders was decreased. This result is consistent with the previous observation that  $\omega_t$  tends to follow the mean tangential velocity in the annulus, since the latter must increase with decreasing  $L$  due to the influence of the endplates.

As a first step in investigating the two-dimensionality of the flow pattern in a helical coordinate system attached to the interfaces, the intermittency factor for  $R_o = -50,000$ ,  $R_i = 5,600$  was measured as a function of axial position for two different radii. Since probes could be installed only at positions 1 ft apart along the cylinders, measurements at intermediate stations were made by moving both end plates in the same direction, keeping the length of the working space fixed. To allow this freedom, it was necessary to reduce the length of the working space to 46.7 in.

The interfaces were found to be sharply defined and stable for all axial locations. The measurements of  $\gamma$ , collected in Figure 10, suggest a useful degree of two-dimensionality in the central region. On the other hand, there are regions at each end, accounting for 40 to 50% of the (shortened) working space, in which significant axial variations may exist.

Several methods have been used to measure the mean shape of the interface pattern in the optimal flow. All of these methods involved the

use of two different hot-wires. In the earliest measurements, the signals from two hot-wires, mounted at different radial locations on a single probe, were added and the interface pattern was inferred from the intermittency factors for the individual and combined signals. This method, unfortunately, was found to be inapplicable to a large fraction of the flow because of the geometrical character of the interface pattern. A different method was therefore adopted, using tape-recorded data\* to determine the average time interval between crossings of a given interface by two hot-wires. One probe was kept fixed at  $r = 17$  in., while the other (located 180-deg from the first) was traversed radially. Since the tapes could be played in either direction, the two interfaces could be observed independently. One residual problem in this method is that the discrimination between laminar and turbulent flow is still being made in terms of fluctuating voltages rather than velocities. With this reservation, the interface-geometry data are shown in Figure 11 in a coordinate system rotating with the mean angular velocity of the turbulence,  $\omega_t$ . The mean cross-section of the turbulent volume of fluid is roughly antisymmetrical around  $r = 17$  in., so that the interface pattern is nearly the same when observed from either of the two cylinders. A tail of turbulent fluid near  $r = 16.5$  in. is stretched out in the direction of motion of the inner cylinder, while a nose near  $r = 17.5$  in. is stretched out in the direction of motion of the outer cylinder. As a byproduct of the measurement of mean interface position, the circumferential dispersion in this position was also measured, with the result shown in Figure 12. Note that the dispersion in the leading interface (i.e., leading

---

\*The tape-recorded data in question are being used to determine mean and fluctuating velocity fields in the optimal spiral turbulence by means of digital sampling methods. A detailed discussion of the turbulence-discrimination and data-handling techniques had been given by Van Atta (1965).



in laboratory coordinates) is considerably smaller at all radii than the dispersion in the trailing interface. This is the first evidence of any significant difference in the structure or behavior of interfaces separating laminar and turbulent regions of the fluid.

#### 8. Time Scale for Fluctuations in Interface Position

The present measurements give no information about the instantaneous shape or velocity of the interfaces. Measurement of instantaneous shape would require the employment of a large number of judiciously placed probes whose wakes would probably seriously modify the mean flow. Measurement of instantaneous velocity at a point on the interface presents a similar difficulty. The magnitude of the characteristic time scale for random fluctuations in interface position, however, was inferred indirectly during the study of mean interface position. Let  $\delta_n = P_n - \langle P \rangle$  denote the deviation from the mean of a single time interval  $P_n$ , whose end points are determined by successive interface crossings. Let  $\delta_{n+\nu}$  denote the corresponding deviation measured  $\nu$  intervals later. From the tape-recorded data, normalized correlations  $\langle \delta_n \delta_{n+\nu} \rangle / \langle \delta_n^2 \rangle$  have been computed for values of  $\nu$  from 1 through 10 for various radii. As shown for one example in Figure 13, the intervals are essentially independent\* (more accurately, the correlation is essentially zero) for  $\nu \geq 2$ . The correlation between adjacent intervals ( $\nu = 1$ ), shown in Figure 14, lies consistently between -0.45 and -0.52 for all radial locations, showing that an interval longer than  $\langle P \rangle$  is likely to be immediately followed by an interval shorter than  $\langle P \rangle$ . In fact, the observed correlations correspond

---

\* This result was first obtained by hand computation for a single case, using a preliminary tape recording (at nearly the same radial location and Reynolds number) and the intermittency meter as described in Section 6.

closely to what would be expected if the characteristic time scale (correlation time) for random fluctuations in interface position were appreciably less than the time  $P_n$  required for the probe to traverse the flow pattern. This assumption implies (see Appendix) that  $\langle \delta_n \delta_{n+1} \rangle / \langle \delta_n^2 \rangle = -0.5$  for  $\nu = 1$  and  $\langle \delta_n \delta_{n+\nu} \rangle / \langle \delta_n^2 \rangle = 0$  for  $\nu \geq 2$ . The observed correlation of  $-0.45$  to  $-0.52$  for adjacent intervals, and the small values of the higher order correlations, are therefore strong evidence that the interface memory or correlation time is appreciably less than  $P_n$ .

#### Appendix A. Serial Correlation for Time Interval Between Successive Observations of a Given Interface

At a fixed radius, the angular position of a given interface in laboratory coordinates  $\theta(t)$  may be decomposed into mean and fluctuating parts. The mean part,  $\omega_t t$  is a linear function of time, while the fluctuating part  $\theta(t)$  is a stationary stochastic function of time with zero mean. Suppose that the measuring probe is mounted on the outer cylinder (the argument is nearly identical for a probe on the inner cylinder). In the time interval,  $P_n = t'_n - t_n$ , between probe crossings of a given interface, the angular distance travelled by the probe is  $\omega_o P_n$ , while the angular distance travelled by the interface is  $\omega_t P_n + \theta(t'_n) - \theta(t_n)$ . Allowing for the fact that the probe traverses the interface at the ends of the interval  $P_n$ , (Figure A-1) then

$$\omega_o P_{n+j} = 2\pi + \omega_t P_{n+j} + \theta(t'_{n+j}) - \theta(t_{n+j})$$

or, since

$$\theta(t_{n+j}) = \theta(t'_{n+j-1})$$

$$\delta_{n+j} = P_{n+j} - \langle P \rangle = \frac{\theta(t_{n+j}) - \theta(t_{n+j-1})}{\omega_o - \omega_t}$$

The normalized correlation between the fluctuation for one interval and the fluctuation for the  $j^{\text{th}}$  following interval is therefore

$$\psi_j = \frac{\langle \delta_n \delta_{n+j} \rangle}{\langle \delta_n^2 \rangle} = \frac{2 \langle \theta(t_n) \theta(t_{n+j}) \rangle - \langle \theta(t_n) \theta(t_{n+j-1}) \rangle - \langle \theta(t_n) \theta(t_{n+j+1}) \rangle}{2 \langle \theta^2(t_n) \rangle - 2 \langle \theta(t_n) \theta(t_{n+1}) \rangle}$$

If the characteristic period of random fluctuations in interface position is negligibly small compared with  $P_n$ , then values of  $\theta(t)$  separated by an interval  $P_n$  or greater will be uncorrelated in the mean, that is

$$\langle \theta(t) \theta(t + T) \rangle = 0; T \geq P_n$$

If this is the case, then

$$\psi_j = \frac{\langle \delta_n \delta_{n+j} \rangle}{\langle \delta_n^2 \rangle} = \begin{matrix} 1 & j = 0 \\ -0.5 & j = 1 \\ 0 & j \geq 2 \end{matrix}$$

These results, which are independent of the distribution function for  $P$ , explain how a strong first order ( $j = 1$ ) correlation and negligible higher-order correlations can obtain when a random variable is observed periodically and, compared with the correlation time for the fluctuations, relatively infrequently.

It has been implicitly assumed, in view of experimental evidence like that in Figure 2, that fluctuations in interface position, although rapid, are slow enough so that the probe may cross each interface only once (always in the same direction) during each encounter with the turbulent volume of fluid. For less regular cases, the interfaces may fluctuate so rapidly that they appear to be poorly defined even though the interface itself remains sharp, and the argument given here might not apply.

## REFERENCES

- Coles, D. 1962 "Interfaces and Intermittency in Turbulent Shear Flow,"  
Mecanique de la Turbulence, CNRS, Paris, 229-248.
- Coles, D. 1965 J Fluid Mech. 21, 385-425
- Coles, D. and Van Atta, C. "Measured Distortion of a Laminar Couette  
Flow by End Effects" (To be published).
- Schultz-Grunow, F. 1959 Z. angew. Math. Mech. 39, 101-110
- Van Atta, C. W. 1964 Ph.D. Thesis, California Institute of Technology

## Table of Symbols

$f_i$	Frequency of interface pattern as observed from inner cylinder
$f_o$	Frequency of interface pattern as observed from outer cylinder
$l_t$	Apparent length of turbulent region at $r = \text{constant}$
$L$	Length of annular working space = distance between end plates
$P$	Time interval between probe crossings of a given interface; $\langle P \rangle \frac{1}{f}$
$\delta$	$P - \langle P \rangle$
$r$	Radial coordinate
$r_i$	Radius of inner cylinder
$r_o$	Radius of outer cylinder
$R_i$	Reynolds number of inner cylinder; $R_i = \frac{\omega_i r_i^2}{\nu}$
$R_o$	Reynolds number of outer cylinder; $R_o = \frac{\omega_o r_o^2}{\nu}$
$z$	Axial coordinate measured from mid-plane of symmetry
$\alpha$	Pitch angle of helix measured with respect to plane $z = \text{constant}$
$\gamma$	Intermittency factor
$\theta$	Fluctuating component of interface position
$\Theta$	Angular coordinate
$\sigma$	Standard deviation of random variable
$\nu$	Kinematic viscosity of air
$\omega_i$	Angular velocity of inner cylinder
$\omega_o$	Angular velocity of outer cylinder
$\omega_t$	Mean angular velocity of spiral turbulence in laboratory coordinates
$\langle \rangle$	Stochastic mean value

- Fig. 1. Spiral turbulence; flow visualization by Coles using suspension of aluminum powder in silicone oil.  $R_o = -15,880$ ,  $R_i = 5,250$
- Fig. 2. Typical hot-wire signal in spiral turbulence.  $R_o = -50,000$ ,  $R_i = 5,600$ . Probe mounted on outer cylinder at  $r = 17.125$  in.
- Fig. 3. Boundary for catastrophic transition. Circles and triangles show position of transition boundary (approached from below). Squares show boundary for permanent disappearance of turbulence (approached from above).
- Fig. 4. Angular velocity  $\omega_t$  of spiral turbulence pattern. Open circles are data for constant  $R_o$ ; solid circles are data for constant  $R_i$ . Dotted line is Taylor boundary. Point A corresponds to photograph in Fig. 1; point B to optimal flow; points C and D to flows studied by Oguro (unpublished).
- Fig. 5. Typical distribution function for interface position at  $r = 17$  in.
- Fig. 6. Standard deviation of interface position at  $r = 17$  in. as function of  $R_i$  for fixed  $R_o = -48,000$ . Data based on 300 cycles of flow for each value of  $R_i$ . Data are for trailing interface (see Figure 11).
- Fig. 7. Variation of  $\gamma$  with  $R_i$  for fixed  $R_o$  (solid circles); radial distribution of  $\gamma$  for  $R_i = 5,600$ ,  $R_o = -50,000$  (open circles).
- Fig. 8. Distribution of observed length of turbulent region at different radii in the optimal flow.
- Fig. 9. Distribution interface position at different radii in a typical spiral turbulent flow.
- Fig. 10. Axial distribution of  $\gamma$  for  $R_o = -50,000$ ,  $R_i = 5,600$ .
- Fig. 11. Mean interface geometry for the optimal flow, with radial scale slightly expanded for clarity. Data based on approximately 3,000 cycles of flow for each point on interface.
- Fig. 12. Standard deviation of interface location for leading and trailing interfaces.

Fig. 13. Example of serial correlation for interval between successive observations of one interface in the optimal flow.

Fig. 14. Correlation for adjacent intervals between successive observations of interface position in the optimal flow.